Silicon Atom Substitution Enhances Interchain Packing in a Thiophene-Based Polymer System

By *Hsiang-Yu Chen, Jianhui Hou, Amy E. Hayden, Hoichang Yang, K. N. Houk,* and *Yang Yang**

Silole-containing organic materials have been known to exhibit altered properties with respect to their carbon analogues.[1–4] Recently, different categories of silole-containing polymers have been reported to show promising characteristics as materials for thin-film transistors[5] and polymer solar cells.[6,7] Most of the previous studies on silole derivatives mainly focus on the molecular orbital shapes and energies.[1–4] How the replacement of a carbon atom by a silicon atom influences the interaction between molecules has not been addressed. Here we compare a silole-containing polymer with its carbon counterpart and show that the material properties, particular the packing of polymer chains, can be altered significantly. As a result, different processing conditions are needed to obtain high-efficiency solar cells. Packing simulations show that the geometrical effect caused by the replacement of the carbon atom with a silicon atom plays a dominant role effecting the polymer stacking property.

Polymer solar cells have the advantages of having lower cost and lighter weight, as well as being fabricated via easier processing methods, when compared with commercial inorganic material-based solar cells. However, most of the current polymer solar cells show power conversion efficiencies (PCE) of less than 5%, mainly due to the low carrier mobilities. Recently an efficient solar cell based on a low bandgap polymer, poly{[4,4-bis(2-ethylhexyl)-cyclopenta-(2,1-b;3,4-b')dithiophene]-2,6-diyl-*alt*-(2,1,3- benzothiadiazole)-4,7-diyl} (PCPDTBT, Scheme 1a) was reported using additives to control the desired morphology.[8] With the reports of the high carrier mobility of silole-containing polymers,[5] attempts to further improve the efficiency of polymer solar cells by transforming PCPDTBT to the silole-containing polymer, poly{[4,4′-bis(2-ethylhexyl)dithieno(3,2-b;2′,3′-d)silole]-2,6-diyl-*alt*-(2,1,3-benzothidiazole)-4,7-diyl} (hereafter referred to as PSBTBT, Scheme 1b), has been recently realized.[7] By replacing the 5-position carbon of PCPDTBT with a silicon atom, a PCE of as high as 5.6%[7] [processed with chloroform, see the Supporting Information (SI), Fig. S1] can be achieved. While trying to optimize solar cells based on PCPDTBT and PSBTBT, we found that very different processing conditions are needed, indicating that the intrinsic material properties of these two polymers are rather different. In this manuscript, we explore experimentally how the silicon influences material properties and device performance, and quantum chemical calculations are used to identify the origin of changes from the carbon analogue.

The polymer solar cells studied here are produced from blend solutions of polymer/$PC_{70}BM$ (see the Experimental section for details). For comparison, PCPDTBT is synthesized by the method reported in the literature[9] and devices based on PCPDTBT/$PC_{70}BM$ (1:3 w/w) show a PCE comparable to the previously reported value (~3.1%, without any additives).[8,9] It has been reported that thermal annealing does not improve the device performance of solar cells based on PCPDTBT.[8] Similarly, we did not observe any efficiency improvement after thermal annealing in our PCPDTBT-based devices. Our previous work[7] showed that the efficiency of polymer solar cells based on the silole-containing polymer, PSBTBT, can be significantly improved from 3.8% to 5.6% by thermal annealing (SI, Fig. S1). To correlate the charge transport property of PSBTBT device with thermal annealing, the change of hole mobility is measured by thin-film transistors (TFT) before and after annealing. The mobility (extracted from the saturation regime; see SI, Fig. S2) obtained after annealing at 140 °C for 5 min is $\sim 3 \times 10^{-3}$ cm^2 V^{-1} s^{-1}, which is approximately five times higher than that before annealing ($\sim 6 \times 10^{-4}$ cm^2 V^{-1} s^{-1}). A mobility higher than 10^{-3} cm^2 V^{-1} s^{-1} is desired for high-efficiency polymer solar cells in order to have efficient charge transport.[10] The increase in mobility after thermal annealing is likely one of the reasons for the increased

[*] Prof. Y. Yang, H. Y. Chen, J. Hou
Department of Materials Science and Engineering
University of California-Los Angeles
Los Angeles, CA 90095 (USA)
E-mail: yangy@ucla.edu
Prof. K. N. Houk, A. E. Hayden
Department of Chemistry and Biochemistry
University of California-Los Angeles
Los Angeles, CA 90095 (USA)
Prof. H. Yang
Department of Advanced Fiber Engineering, Inha University
Yonghyun-dong 253, Incheon 402-751 (Korea)

DOI: 10.1002/adma.200902469

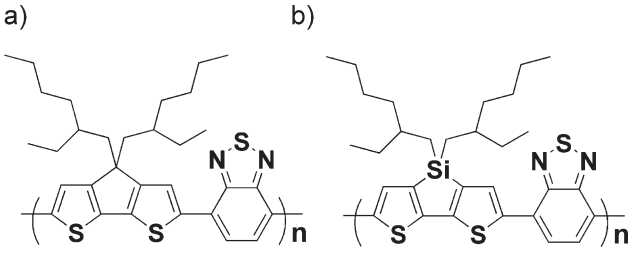

Scheme 1. Structure of a) PCPDTBT and b) PSBTBT. By replacing the 5-position carbon of PCPDTBT with a silicon atom, a silole-containing polymer with high crystallinity (PSBTBT) is obtained.

© 2009 WILEY-VCH Verlag GmbH & Co. KGaA, Weinheim

Final page numbers not assigned

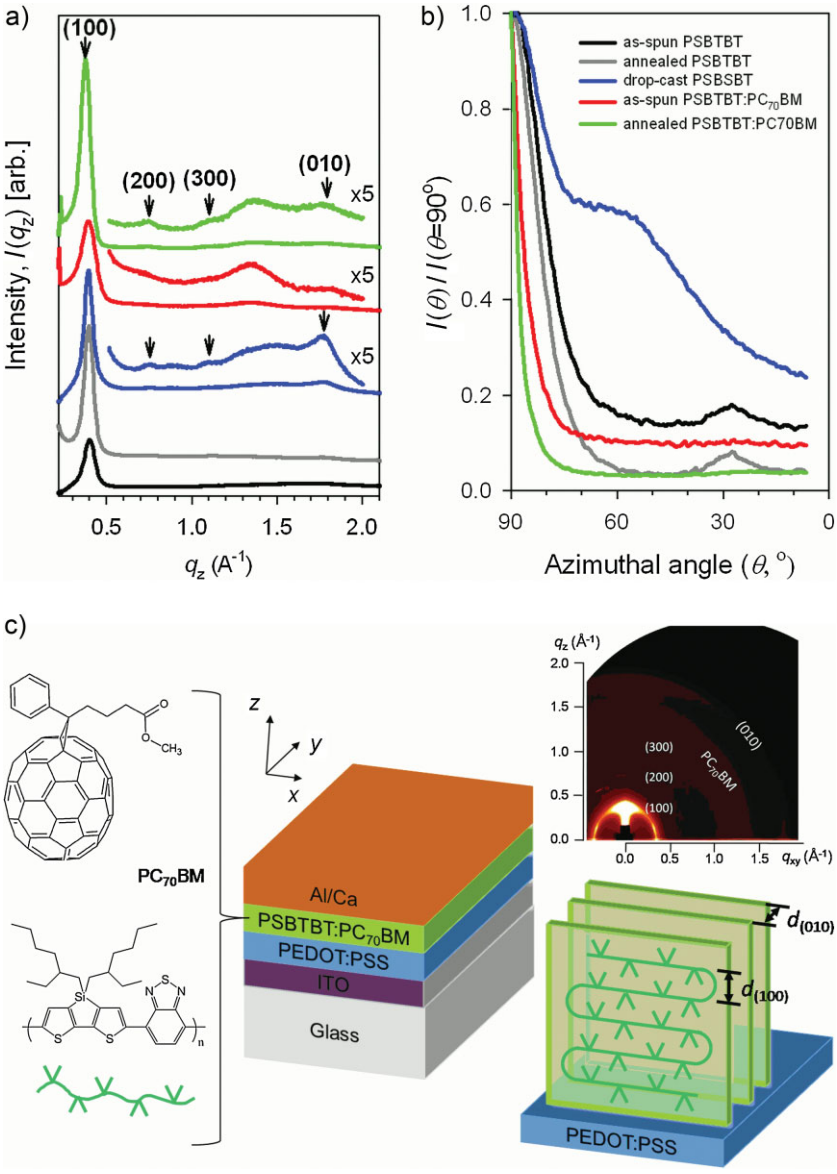

Figure 1. a) Out-of-plane and b) azimuthal scan (at $q^{(100)}$) X-ray profiles of PSBTBT and PSBTBT/$PC_{70}BM$ films. These X-ray profiles were extracted 2D GIXD patterns measured at an incident beam angle of 0.15°. c) Schemes of the PSBTBT/$PC_{70}BM$-based solar cell device; after annealing, PSBTBT chains form highly oriented edge-on structures on the PEDOT:PSS surface, indicating that the orientation of the π–π stacking planes is parallel to the surface (see bottom right corner), as determined by its 2D GIXD pattern (see upper right corner).

short-circuit current density (J_{sc}, increased from −10.9 to −13.6 mA cm^{-2}) and fill factor (FF, from 50.9% to 62.2%), both of which contribute to the high efficiency. Tapping-mode atomic force microscopy (AFM) was then used to study the nanoscale morphology change before and after annealing (see SI, Fig. S3). However, no obvious change was observed after thermal annealing. A stronger interaction between polymer molecules after thermal annealing is thus suspected to be the reason for the increase in carrier mobility. The discernible response to thermal annealing after replacing the 5-position carbon of PCPDTBT with a silicon atom demonstrates the different self-assembly characteristics of these two polymers.

To clarify the nature of the molecular stacking by PSBTBT, grazing incidence X-ray diffraction (GIXD) was used to investigate the crystalline structures of both PSBTBT and PSBTBT/$PC_{70}BM$ blend films on PEDOT:PSS/ITO/glass substrates. It is known that the ITO layer of a multilayered substrate can show strong powder-like X-ray reflections. To exclude the reflection from ITO, the 2D GIXD patterns were extracted using background patterns from the substrate (see SI, Fig. S4). Out-of-plane (Fig. 1a) and azimuthal angle X-ray profiles (Fig. 1b) were then extracted from these 2D GIXD patterns to systematically investigate the crystalline structure of PSBTBT. In the out-of-plane X-ray profiles (Fig. 1a), pure PSBTBT films before (black line) and after (gray line) annealing show an intense peak at $q_z \sim 0.404$ Å^{-1}, corresponding to the reflection of (100) crystal planes (see Fig. 1c) with an interlayer spacing $d_{(100)}$ of ~15.5 Å. The much stronger peak intensity after annealing is related to the increase in film crystallinity,[11] which is consistent with the observed thickness variation of ~15%. In contrast, drop-cast PSBTBT films fabricated with a longer solvent evaporation time of ~5 min (through the use of chlorobenzene, CB) show much stronger out-of-plane X-ray reflections of (100) with higher order planes (blue line). The (010) crystal planes, which are oriented normal to the (100) planes, are also detected with an estimated $d_{(010)}$ (π-stacking spacing) of ~3.48 Å. These results suggest that the slow solvent evaporation process aids in the growth of highly crystalline but randomly oriented PSBTBT crystals with respect to the surface normal. To the best of our knowledge, such short $d_{(010)}$ has not been observed in other self-assembled semiconducting polymers, e.g., $d_{(010)}$ is ~3.8 Å for poly(3-hexylthiophene) (P3HT).

Similar to what is observed with pure PSBTBT films, the long-range ordering of PSBTBT crystals in the blend with $PC_{70}BM$ is enhanced by thermal annealing (green line). By comparing annealed PSBTBT (Fig. 1, gray line) with annealed blend film (green line), the increase in the X-ray reflection ratio of the (100) to (010) plane in the annealed blend film strongly supports the hypothesis that the edge-on[12,13] orientation of PSBTBT is enhanced by the presence of $PC_{70}BM$ in the blend system (Fig. 1c), as also determined by the azimuthal scan profiles of these films (Fig. 1b). In addition, the PSBTBT/$PC_{70}BM$ film shows a discernible change in $d_{(100)}$ before (15.5 Å) and after (16.7 Å) thermal annealing, indicating that some portion of the $PC_{70}BM$ molecules diffuse into the space between the intertwining side-chain groups along the π–π conjugated planes.[14]

On the other hand, no indication of crystallization was observed in the PCPDTBT system with or without additives, as

WILEY InterScience® DISCOVER SOMETHING GREAT
© 2009 WILEY-VCH Verlag GmbH & Co. KGaA, Weinheim

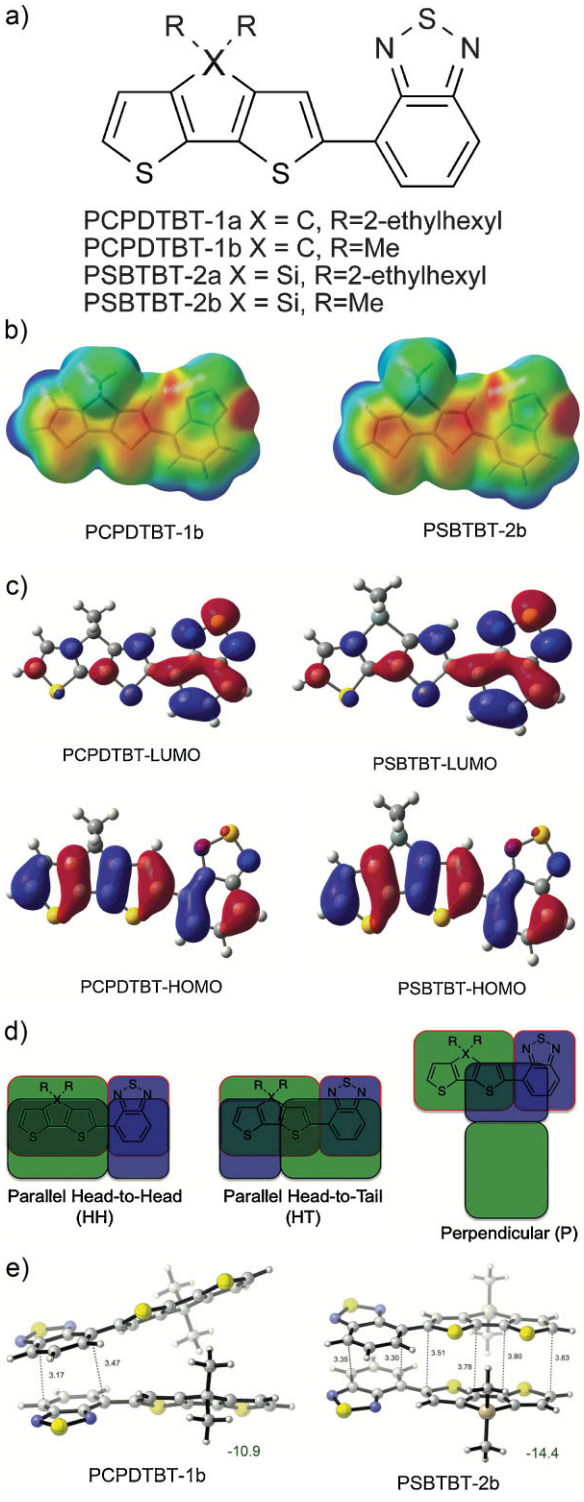

Figure 2. a) Structures of the model systems for PCPDTBT and PSBTBT used in computations. b) Electrostatic potential maps and c) HOMOs and LUMOs computed with B3LYP/6-31G(d). d) Orientations of subunit dimers considered in the computations. These three orientations were obtained from force field conformational searches, and were used in subsequent quantum mechanical calculations. e) Structures of the head-to-head dimers. Binding energies (green) are given in kcal mol^{-1}. Distances are shown in Å.

also was previously reported by Peet et al.[8] The significant change from an amorphous material to a crystalline material by replacing the carbon at the 5-position of PCPDTBT with a silicon atom suggests that the interactions between the polymer molecules in these two materials are very different. Silole-containing organic materials have been studied for a long time because of their interesting properties when compared with their carbon analogues.[1–4] Because the silicon has relatively low-lying σ^* orbitals,[15–17] the silicon atom can enter into π-conjugation with the diene, which gives rise to a lower lowest unoccupied molecular orbital (LUMO) in the silole analogue.[2,5]

To gain insight into the electronic properties and molecular interactions of both PCPDTBT and PSBTBT, computations were then performed with several different computational methods. First, conformational searches with a force field model, using a Monte Carlo algorithm were performed on monomeric units of each polymer (PCPDTBT-**1a** and PSBTBT-**2a**, Fig. 2a) using the OPLS-AA force field with the GB/SA solvation model for chloroform in Macromodel.[18] This procedure provides many different conformers and then approximates their relative energies. The low energy conformers were then subjected to density functional theory (DFT) optimizations using the B3LYP[19] functional with the 6-31G(d) basis set in Gaussian03 (see SI, Fig. S5).[20] This quantum mechanical method gives relatively accurate energetics. According to these DFT computations, the conformation shown in Figure 2a with the thiadiazole ring syn to the alkyl substituents is preferred by ~1 kcal mol^{-1} for both units.

After determining the favored conformation of these monomers, the long alkyl chains were substituted by methyl groups in order to shorten computation time (PCPDTBT-**1b** and PSBTBT-**2b**). B3LYP computations of the electrostatic potential (ESP) surface (Fig. 2b) and the bandgaps (2.61 and 2.69 eV, respectively) showed that both have very similar ESPs and bandgaps. In addition, the highest-occupied molecular orbitals (HOMOs) and LUMOs are similar for both molecules (Fig. 2c). Together, these results indicate that a significant difference in the electronic structures of the C and Si analogues is not predicted for these systems.

The intermolecular interactions between two PCPDTBT-**1b** or PSBTBT-**2b** units were explored first with conformational searches on the dimers. Three types of dimers are found to be low in energy: 1) parallel head-to-head (HH), 2) parallel head-to-tail (HT), and 3) perpendicular complexes (P), which are shown schematically in Figure 2d. All three types of dimer structures for both the carbon and silicon analogues were optimized using a DFT method known to give reasonable π-complexation energies,[21] MO5-2X[22] in the program Gamess.[23] Many of these dimers were found to have similar complexation energies of around −10 kcal mol^{-1} (see SI, Fig. S6). However, the HH orientation for the PSBTBT monomer is predicted to have a significantly more favorable complexation energy of −14 kcal mol^{-1} (Fig. 2e). For this dimer, a parallel geometry is predicted with an averaged $d_{(010)}$ (π-stacking spacing) of 3.56 Å, which is very close to the value observed from GIXD (~3.48 Å). In the HH orientation, PCPDTBT is unable to adopt a parallel geometry (Fig. 2e), presumably as a result of steric interactions between the methyl groups in this model system and the long alkyl chains in the polymer. The C−Si bond is

© 2009 WILEY-VCH Verlag GmbH & Co. KGaA, Weinheim

Final page numbers not assigned

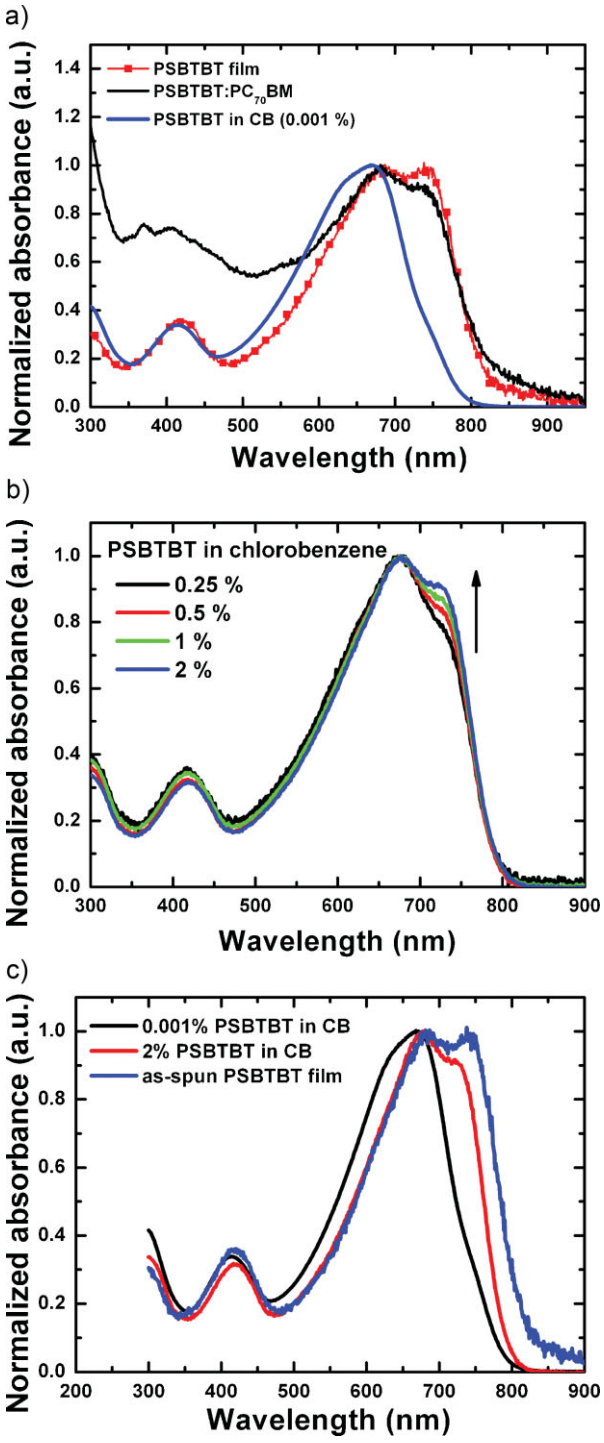

Figure 3. a) Absorption spectra of PSBTBT in dilute solution and in solid film. The large red-shift of the absorption edge of pure PSBTBT from solution to solid film suggests strong interchain interaction in solid state. b) Absorption spectra of PSBTBT solutions with different concentrations. The growth of the π–π interaction peak at ~725 nm with increasing concentrations is clearly seen. c) Absorption spectra of PSBTBT in different states. Absorption spectra of PSBTBT in very dilute solution (0.001% in CB), higher concentration solution (2% in CB, the concentration used to make devices), and in solid state (as-spun film), show different levels of π–π interaction of PSBTBT molecules.

significantly longer than the C–C bond (1.89 and 1.53Å, respectively), allowing more efficient packing due to the absence of steric hindrance between the alkyl groups and the thiophene rings.

According to the results of the simulation, strong intermolecular interactions between PSBTBT molecules are expected. From the absorption spectra, a significant red shift of the absorption edge of PSBTBT from solution (0.001% in CB, blue line) to the solid state (spin-coated film) is observed (Fig. 3a), suggesting strong intermolecular interactions in the solid state.[24] The absorption peak of the PSBTBT film at ~740 nm is attributed to the strong π–π interaction of PSBTBT molecules (see SI, Fig. S7). As a result, the intensity of the peak at 740 nm slightly decreases in the presence of $PC_{70}BM$ (Fig. 3a, black line). With the speculation of interaction of polymer molecules in the solution state, solutions with different concentrations were produced and the absorption spectra (see the Experimental section for details) are shown in Figure 3b. The growth of the π–π interaction peak with increasing concentration of PSBTBT is clearly seen, indicating that, at a concentration of 2% (20 mg mL^{-1} PSBTBT, the concentration used to make solar cell devices), strong π–π interaction already occurs in the solution state. Different levels of π–π interaction are observed in different concentrations of solutions and the solid (film) state (Fig. 3c). The slight shift of the major peak at ~670 nm from solution to solid state (Fig. 3c) suggests that the backbone of PSBTBT is rather planar (less twisted) even in solution state, which is consistent with the conformational simulation results.

In conclusion, a new silole-containing low bandgap polymer was synthesized by replacing the 5-position carbon of PCPDTBT with a silicon atom (PSBTBT). With this subtle difference in the chemical structures of these two polymers, their response toward thermal treatment is, however, rather different. Therefore, the interactions between polymer molecules are studied via experiments as well as by computational calculations. By measuring the hole mobility of PSBTBT with thin film transistors, it was found that the hole mobility is five times higher after annealing. From the simulation results, the C–Si bond is significantly longer than the C–C bond, which reduces the steric hindrance from the bulky alkyl groups. As a result, the polymer changes from an amorphous (PCPDTBT) to a highly crystalline (PSBTBT) structure, as characterized by GIXD. Under thermal treatment, the crystallinity of the PSBTBT solid films can be effectively improved, which results in a higher carrier mobility. Strong π–π stacking is even observed in the solution. No significant difference is found in the electronic structures by the replacement of the carbon atom by a silicon atom. This discovery highlights subtle differences in monomer structure that can have a profound influence on intermolecular interactions, a perspective that has implications for future polymer design.

Experimental

PSBTBT was synthesized using the method reported in Ref. [7] and $PC_{70}BM$ was purchased from Nano-C (used as received). Both PSBTBT and $PC_{70}BM$ were then dissolved in chloroform in a 1:1.5 (10 mg mL^{-1}:15 mg mL^{-1}) wt. ratio. The solutions were spin-coated on ITO (indium tin oxide)/glass substrates with a pre-coated PEDOT/PSS [poly(ethylenedioxythiophene)/

WILEY InterScience® DISCOVER SOMETHING GREAT
© 2009 WILEY-VCH Verlag GmbH & Co. KGaA, Weinheim

polystyrene sulfonate] layer. The PSBTBT:$PC_{70}BM$ films were spin-coated at 5000 rpm and the thicknesses before and after annealing were approximately 100 and 85 nm, respectively. A bilayer electrode composed of calcium (Ca, 20 nm) and aluminium (Al, 100 nm) was then thermally evaporated on top of the polymer films. The device active area was $\sim$0.12 cm^2 for all the solar cell devices discussed in this work. Device characterization was performed in an N_2 atmosphere under simulated AM1.5G irradiation (100 mW cm^{-2}) using a xenon lamp-based solar simulator (Oriel 96000 150 W Solar Simulator) [25].

The absorptions spectra of the solutions shown in Figure 3b and 3c were taken by drop-casting the solutions onto a glass substrate and then covering it by another piece of glass so that the behavior of polymer molecules in the solution could be imitated.

Thin-film transistors (TFT) of PSBTBT were fabricated by spin-coating PSBTBT film (with 1% PSBTBT in CB) onto pre-cleaned SiO_2 (300 nm)/Si substrates. Bottom contact devices were comprised of chromium (Cr, 10 nm)/gold (Au, 40 nm) as the source and drain electrodes, respectively, with $W = 500\ \mu m$ and $L = 25\ \mu m$ (also see the Supporting Information).

Acknowledgements

H.Y.C. and Y.Y. acknowledge the financial support from Solarmer Energy Inc. (grant number 20061880) and UC Discovery Grant (GCP05-10208). H.Y.C. acknowledges the assistance of Wei Lek Kwan, Teresa Chen, and Guanwen Yang on the experiments. The valuable discussions with Dr. Gang Li of Solarmer Energy Inc. are also highly appreciated. H.Y. acknowledges the United States Department of Energy, Office of Basic Energy Sciences (DE-AC02-98CH10886) for providing the National Synchrotron Light Source facilities for use in this work and the financial support from the Nanoscale Science and Engineering Institute of the National Science Foundation (DMR 0117792). A.E.H. and K.N.H. acknowledge the National Science Foundation for financial support (CHE-0548209) and the UCLA Academic Technology Services for computing resources. Supporting Information is available online from Wiley InterScience or from the author.

Received: July 1, 2009
Published online:

[1] D. M. Wetzel, J. I. Brauman, *J. Am. Chem. Soc.* **1988**, *110*, 8333.
[2] S. Yamaguchi, K. Tamao, *Bull. Chem. Soc. Jpn.* **1996**, *69*, 2327.
[3] X. Zhan, C. Risko, F. Amy, C. Chan, W. Zhao, S. Barlow, A. Kahn, J.-L. Bredas, S. R. Marder, *J. Am. Chem. Soc.* **2005**, *127*, 9021.
[4] C. Risko, G. P. Kushto, Z. H. Kafati, J. L. Bredas, *J. Chem. Phys.* **2004**, *121*, 9031.
[5] G. Lu, H. Usta, C. Risko, L. Wang, A. Facchetti, M. A. Ratner, T. J. Marks, *J. Am. Chem. Soc.* **2008**, *130*, 7670.
[6] E. Wang, L. Wang, L. Lan, C. Luo, W. Zhuang, J. Peng, Y. Cao, *Appl. Phys. Lett.* **2008**, *92*, 033307.
[7] J. Hou, H.-Y. Chen, S. Zhang, G. Li, Y. Yang, *J. Am. Chem. Soc.* **2008**, *130*, 16144.
[8] J. Peet, J. Y. Kim, N. E. Coates, W. L. Ma, D. Moses, A. J. Heeger, G. C. Bazan, *Nat. Mater.* **2007**, *6*, 497.
[9] Z. Zhu, D. Waller, R. Gaudiana, M. Morana, D. Muhlbacher, M. Scharber, C. Brabec, *Macromolecules* **2007**, *40*, 1981.
[10] M. C. Scharber, D. Muhlbacher, M. Koppe, P. Denk, C. Waldauf, A. J. Heeger, C. J. Brabec, *Adv. Mater.* **2006**, *18, 789*.
[11] H. C. Yang, T. J. Shin, L. Yang, K. Cho, C. Y. Ryu, Z. N. Bao, *Adv. Funct. Mater.* **2005**, *15*, 671.
[12] H. Sirringhaus, P. J. Brown, R. H. Friend, M. M. Nielsen, K. Bechgaard, B. M. W. Langeveld-Voss, A. J. H. Spiering, R. A. J. Janssen, E. W. Meijer, P. Herwig, D. M. de Leeuw, *Nature* **1999**, *401*, 685.
[13] G. Li, Y. Yao, H. Yang, V. Shrotriya, G. Yang, Y. Yang, *Adv. Funct. Mater.* **2007**, *17*, 1636.
[14] Y. Kim, S. Cook, S. M. Tuladhar, S. A. Choulis, J. Nelson, J. R. Durrant, D. D. C. Bradley, M. Giles, I. McCulloch, C. S. Ha, M. Ree, *Nat. Mater.* **2006**, *5*, 197.
[15] Y. Yamaguchi, *Mol. Eng.* **1994**, *2*, 311.
[16] K. Tamao, S. Yamaguchi, Y. Ito, Y. Matsuzaki, T. Yamabe, M. Fukushima, S. Mori, *Macromolecules* **1995**, *28*, 8668.
[17] C. Guimon, G. Pfister-Guillouzo, J. Dubac, A. Laporterie, G. Manuel, H. Iloughmane, *Organometallics* **1995**, *4*, 636.
[18] V. Maestro, MMshare Version 1.1.018, Schrödinger, L.L.C. **2003**.
[19] P. J. Stephens, F. J. Devlin, C. F. Chabalowski, M. J. Frisch, *J. Phys. Chem.* **1994**, *98*, 11623.
[20] Gaussian 03, Revision C.02, M. J. Frisch, G. W. Trucks, H. B. Schlegel, G. E. Scuseria, M. A. Robb, J. R. Cheeseman, J. A. Montgomery, Jr, T. Vreven, K. N. Kudin, J. C. Burant, J. M. Millam, S. S. Iyengar, J. Tomasi, V. Barone, B. Mennucci, M. Cossi, G. Scalmani, N. Rega, G. A. Petersson, H. Nakatsuji, M. Hada, M. Ehara, K. Toyota, R. Fukuda, J. Hasegawa, M. Ishida, T. Nakajima, Y. Honda, O. Kitao, H. Nakai, M. Klene, X. Li, J. E. Knox, H. P. Hratchian, J. B. Cross, V. Bakken, C. Adamo, J. Jaramillo, R. Gomperts, R. E. Stratmann, O. Yazyev, A. J. Austin, R. Cammi, C. Pomelli, J. W. Ochterski, P. Y. Ayala, K. Morokuma, G. A. Voth, P. Salvador, J. J. Dannenberg, V. G. Zakrzewski, S. Dapprich, A. D. Daniels, M. C. Strain, O. Farkas, D. K. Malick, A. D. Rabuck, K. Raghavachari, J. B. Foresman, J. V. Ortiz, Q. Cui, A. G. Baboul, S. Clifford, J. Cioslowski, B. B. Stefanov, G. Liu, A. Liashenko, P. Piskorz, I. Komaromi, R. L. Martin, D. J. Fox, T. Keith, M. A. Al-Laham, C. Y. Peng, A. Nanayakkara, M. Challacombe, P. M. W. Gill, B. Johnson, W. Chen, M. W. Wong, C. Gonzalez, J. A. Pople, Gaussian, Inc. Wallingford CT: **2004**.
[21] S. E. Wheeler, K. N. Houk, *J. Am. Chem. Soc.* **2008**, *130*, 10854.
[22] Y. Zhao, D. G. Truhlar, *Org. Lett.* **2006**, *8*, 5753.
[23] M. W. Schmidt, K. K. Baldridge, J. A. Boatz, S. T. Elbert, M. S. Gordon, J. H. Jensen, S. Koseki, N. Matsunaga, K. A. Nguyen, S. J. Su, T. L. Windus, M. Dupuis, J. A. Montgomery, *J. Comp. Chem.* **1993**, *14*, 1347.
[24] P. J. Brown, D. S. Thomas, A. Kohler, J. S. Wilson, J. S. Kim, C. M. Ramsdale, H. Sirringhaus, R. H. Friend, *Phys. Rev. B* **2003**, *67*, 16.
[25] V. Shrotriya, G. Li, Y. Yao, T. Moriarty, K. Emery, Y. Yang, *Adv. Funct. Mater.* **2006**, *16*, 2016.

© 2009 WILEY-VCH Verlag GmbH & Co. KGaA, Weinheim